Metallurgy and materials
Metalurgia e materiais

Analysis of precipitate density of an aluminium alloy by TEM and AFM

http://dx.doi.org/10.1590/0370-44672016690019

Sheila Cristina Jacumasso
Aluna de mestrado
Universidade Estadual de Ponta Grossa – UEPG
Departamento de Engenharia de Materiais
Ponta Grossa – Paraná – Brasil
sheijacumasso@gmail.com

Juliana de Paula Martins
Professora Adjunta
Universidade Tecnológica Federal do Paraná - UTFPR
Departamento de Engenharia Química
Ponta Grossa – Paraná – Brasil
julianamartins@utfpr.edu.br

André Luís Moreira de Carvalho
Professor Adjunto
Universidade Estadual de Ponta Grossa - UEPG
Departamento de Engenharia de Materiais
Ponta Grossa – Paraná – Brasil
andrelmc@uepg.br

Abstract

The quantification of nanometric precipitates in Al-Zn-Mg-Cu alloys has been performed by a series of experimental techniques. Especially in the AA7050 alloy, after ageing heat treatment, the particles responsible for the hardening become very thin. Typically, these precipitates of nanometric sizes are mainly characterized by transmission electron microscopy (TEM), which in this particular case, requires a very meticulous preparation. This study investigated a possible alternative quantification of the precipitates by atomic force microscopy (AFM) to complement the technique by TEM. For this, three conditions for heat treatment of an aged aluminium alloy AA7050 were therefore chosen to produce different density and sizes of precipitates. The experimental results showed that the AFM technique proved to be a valid qualitative tool and may complement the results obtained by TEM an exploratory analysis for the microstructures.

Keywords: aluminium alloy AA7050, interrupted ageing, secondary precipitation, TEM and AFM.

1. Introduction

In the 7XXX series alloy, the base Al-Zn-Mg-Cu, is widely used in the aircraft industry. The mechanical strength of these alloys is increased through precipitation of a fine dispersed phase through a heat treatment process called precipitation ageing. Consequently, Guinier-Preston (GP) zones and the η' ($MgZn_2$) and η ($MgZn_2$) precipitates are the main phases present in alloys of the 7XXX series, and the η' phase is primarily responsible for the increased resistance. The sequence of precipitation for alloys of Al-Zn-Mg-Cu is generally summarized as: supersaturated solid solution (SSSS) → GP zones → intermediate precipitates η' → equilibrium precipitates η (Berg *et al*., 2001; Katgerman and Eskin, 2003; Sverdlin, 2003).

The nucleation of these precipitates can occur homogeneously (uniform and non-preferential) and heterogeneously (preferential) in specific places such as grain boundaries, dislocations and vacancies. The size, morphology and distribution of precipitates can result in improvements in the mechanical properties (Katgerman and Eskin, 2003; Andreatta, 2004; Brent *et al*., 2004; Smallman and Ngan, 2007). Temperature and ageing time are the main parameters for the variation in the final formation of precipitates. This precipitation can be carried out only in a simple ageing stage (condition T6), in multiple steps at different times and temperatures, called double ageing (T7451 condition), or by secondary precipitation ageing known in the T6 condition as interrupted followed by ageing for long periods at temperatures around 65 °C, as well as the so-called reversal treatment and re-ageing.

The quantification of these precipitated particles in metallic alloys has been made by a series of characterization techniques, especially by transmission electronic microscopy and scanning electronic microscopy (TEM and SEM). The technique that is most utilized to characterize nanometrics precipitates is the TEM. Unfortunately, this technique requires a careful sample preparation to obtain a very thin substrate, smaller than 100 nm. In articles written by La Garza *et al*. (2002) and Garcia - Garcia *et al*. (2014), the use of atomic force microscopy (AFM) shows evidences of the quantification of the η' and η precipitates with the collaboration of microscopy techniques (TEM and SEM). AFM is little explored regarding the characterization of the microstructure of metallic alloys.

Therefore, with the objective to explore the AFM technique, the present work made a correlation between results of surface roughness in AFM with the density of a precipitated phase in matrix on an AA7050 aluminium alloy obtained by TEM. Three different conditions of ageing heat treatment were chosen to produce different

densities of the precipitated phase in an aluminium alloy matrix: one was overageing and two, underageing:

1) the condition as received T7451 (overageing with double ageing);
2) T6 (underaged condition with simple ageing); and
3) T6I4-65 (underaged condition with interrupted ageing).

2. Experimental procedure

Samples were prepared from a plate of aluminium AA7050-T7451 supplied by Embraer S.A. The chemical composition of this alloy in T7451 as received condition is described in Table 1. Samples were taken in the rolling direction and along its thickness.

Table 1
Chemical composition (wt.%) of AA7050 alloy used in this research.

Zn	Mg	Cu	Zr	Fe	Si	Cr	Mn	Al
5.59	1.87	2.01	0.13	0.07	0.03	0.0004	0.015	Balance

The heat treatment was performed in the following sequence: solution heat treatment (485 °C for 4 hours), quench in water and ageing. The T6 condition is a simple process of ageing; the sample was solubilized and aged at a temperature of 130 °C for 2 hours. The T6I4-65 condition is an interrupted condition; the sample was carried out in two stages. The first ageing step was performed at temperature 130 °C for 30 min. The second stage of ageing was performed at a temperature of 65 °C for 24 hours. The T7451 condition was analysed as received condition, as shown in Table 2. The ageing times and temperatures applied in T6I4-65 and T6 conditions are described in Table 2. These features were based on the studies of Buha *et al.* (2008).

Table 2
Description of ageing heat treatments.

Ageing Heat treatment	Solution treatment	First step	Second step
T7451	485°C for 4h	as received	as received
T6		Ageing at 130°C for 120 min	-
T614-65		130°C for 30min	Ageing at 65°C for 24 hours

To analyse the thin disks for TEM, a TECNAI G2F20 brand device was used. The samples were sanded and polished with the polishing ionic low temperature to avoid heating of the samples and to obtain a thin disk of approximately 100 nm, which is ideal for this type of analysis.

The samples were analysed under atomic-force microscopy (AFM). All samples were studied under a Shimadzu SPM-9600 microscope with 400 nm minimum resolution, equipped with a 125 µm scanner operating in non-contact mode. Small samples were cut and sanded with water silicon carbide-based (SiC) sandpaper and polished with alumina 1 and 0.3 µm, and then etched with Keller's reagent (HF 2 ml, HCl 3 ml, HNO_3 5 ml, H_2O 190 ml). The samples were immerged into Keller's reagent during 10 seconds at room temperature. After this, the samples were cleaned with water and isopropyl alcohol.

In the present work, firstly the precipitate feature was identified through its morphology, distribution and size using TEM analysis according to references. Thus, the precipitate size was measured with AFM analysis for three conditions. In this way, once measured the precipitate size, the same was classified and compared with the TEM analysis and then identified. Moreover, to measure the precipitate size from the 2D AFM image analysis, ImageJ software was used. This software permits the conversion of a known distance in (µm) to distance pixels to be able to measure the precipitate length for the three conditions investigated.

3. Results and discussion

It was possible to identify the GP zone, η' and η phases based on literature (Berg *et al.*, 2001; Buha *et al.*, 2008; Garcia *et al.*, 2014). The GP zones presented in T6 and T6I4-65 conditions are small clusters of atoms coherent with the aluminium matrix. $MgZn_2$ (η' and η) is identified as precipitates that have a size between 1 and 100 nm and intermetallic particles that have a size between 1 and 20 µm (Andreatta, 2004), which are also present in all the three conditions. The TEM microstructural analysis identified the size, morphology, distribution and chemical composition of these phases. In the analysis by TEM, it was possible to assess which condition showed a higher density of hardening phases. Hence, the results obtained by TEM served as a basis for the analysis of the density of precipitates, obtained through surface roughness by AFM.

Figure 1 (a) and (b) obtained in bright field shows the microstructure with artificial ageing heat treatment in the T7451 condition. In Figure 1 (a), second phase particles can be observed in the grain boundaries, as within the matrix, the presence of η precipitate is noted and a region where particles are not observed along the grain boundary are identified in the precipitate free zone (PFZ) about the size of 80 nm. A distinct precipitate-free zone is evident near the grain boundaries (Epler, 2004).

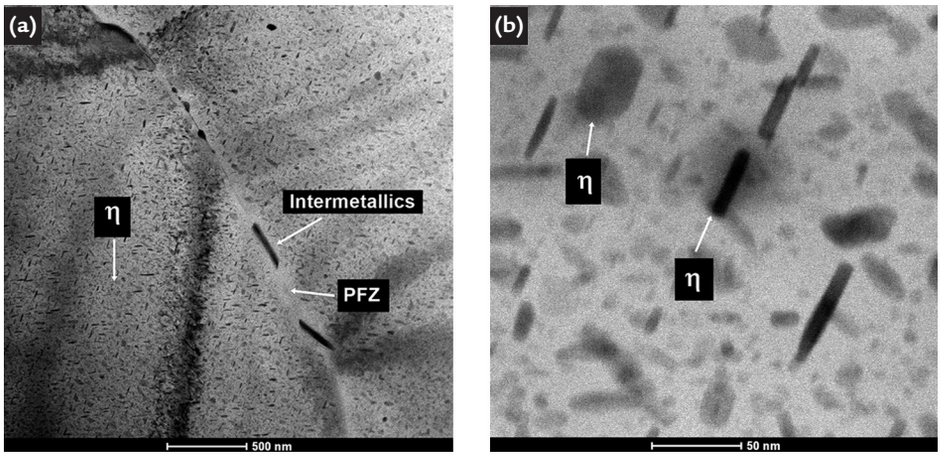

Figure 1
TEM micrograph in bright field (BF) (a) microstructure of alloy AA7050 in artificially aged condition T7451 with second phase particles precipitating in the grain boundaries and within the matrix; (b) a fine distribution of precipitates within the aluminium matrix and the respective morphologies of platelets and needles.

A microstructure with a distribution of nanometric precipitates is shown in Figure 1 (b). The η phases are primarily formed in the regions of defects such as grain boundaries, generating evidence for identification. The structures formed inside the grain have predominantly η stable phase morphology, which have platelets and needles (Brent *et al*, 2004; Epler, 2004). Note the aligned particles are quite spaced, showing low density of precipitates with an average size of the precipitates in the form of platelets around 38 nm and 42 nm for needles. In this overaged condition, it is not possible to notice the presence of GP zones and η' that have been transformed into a more stable phase, η.

Figure 2 (a) and (b) shows a micrograph by TEM in the aged sample T6 condition. This condition presents a PFZ region of approximately 60 nm formed adjacent to the grain boundary, characterized by lack of precipitates. Figure 2 (a) shows grains of various sizes, and the presence of large amounts of precipitates in both grain boundary and inside the matrix. Also note that the fine precipitates are present inside the grains and the size of precipitates is higher in the grain boundary. Precipitates formed at high-angle grain boundaries are usually in the equilibrium phase (η) and larger than those formed in the matrix (η'), owing to preferred nucleation and accelerated growth, due to faster diffusion of solute along grain boundaries than in the matrix (Rometsch *et al*.,2014).

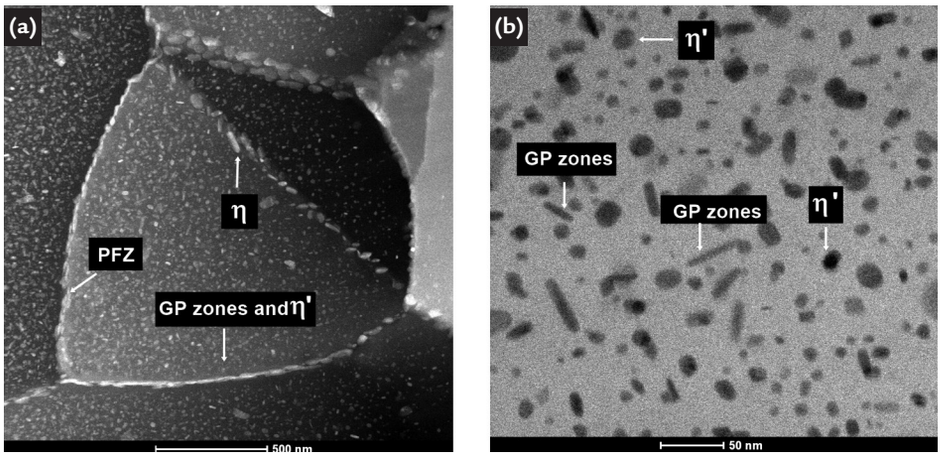

Figure 2
TEM micrographs in artificially aged condition T6: (a) dark field (DF) showing the variation in grain size and nanometric precipitation at the grain boundaries and within the matrix; (b) bright field (BF) showing a fine distribution of precipitates and GPII zones within the aluminium matrix.

The fraction volume of precipitates in the T6 condition consists in a great quantity of GPII zone phases, also η' semicoherent phase, as shows Figure 2 (b). According Buha *et al*. (2008) and Berg *et al*. (2001) GPII zones are formed by one or a few rich Zn-rich atomic layers on $\{1\ 1\ 1\}_{Al}$ and exhibit a plate-like or needle morphology. The metastable coherent η′ phase exhibit a platelets morphology. GPII zones are thinner and often also longer than the η′ phase. It is was found that the approximate size of the needle particles is 23 nm and the platelets is approximately 17 nm. The T6 is an underaged condition, which indicates a transition phase in GPII zones for the formation of the η' phase.

In Figure 3 (a), the ageing microstructure interrupted T6I4-65 condition is obtained in dark field. It is possible to notice in Figure 3 (a) a high density of GPII zones and precipitated inside the grains and at grain boundaries. The T6I4-65 temper increases the density of the η' platelets in alloy 7050 compared to the T6 temper (Buha *et al*., 2008). The TEM observations showed that the precipitates formed in the interrupted peak-aged microstructures were finer, more densely distributed, more closely spaced, and present in greater numbers than they were following the T6 temper (Buha *et al*., 2006). Precipitates observed in Figure 3 (b) present in the grain boundary are possibly of η equilibrium phase, evidenced by their size of around 32 nm and needle morphology. PFZ observes a region of approximately 25 nm, near the grain boundary, characterized by the absence of precipitates. Inside the grain, there is a predominance of GPII zones. It is possible to notice a significant presence of coherent clusters identified as precursor GPII zones of the metastable phase η', which is present in about the size of 14 nm. That is, within the aluminium matrix, there is a predominance of a thin homogeneous distribution of precipitates of nanometric size with a high volume fraction of phase transition to GPII zones η'.

The TEM microstructure obser-

vation for conditions T7451, T6 and T6I4-65 showed that the density and size of the precipitates were significantly different between the three ageing treatment conditions, as can be seen in Figure 4. Thus, one of the objectives was achieved as expected in work; that is, a difference in the density and size of the precipitates.

Consequently, the results of analyses carried out in the T7451 condition showed the predominance of a η phase, about the size of 40 nm, due to the fact of being an overaged condition. Whereas, the T6 condition showed up as underaged, as it showed the presence of GPII zones and η', with approximate sizes of 20 nm.

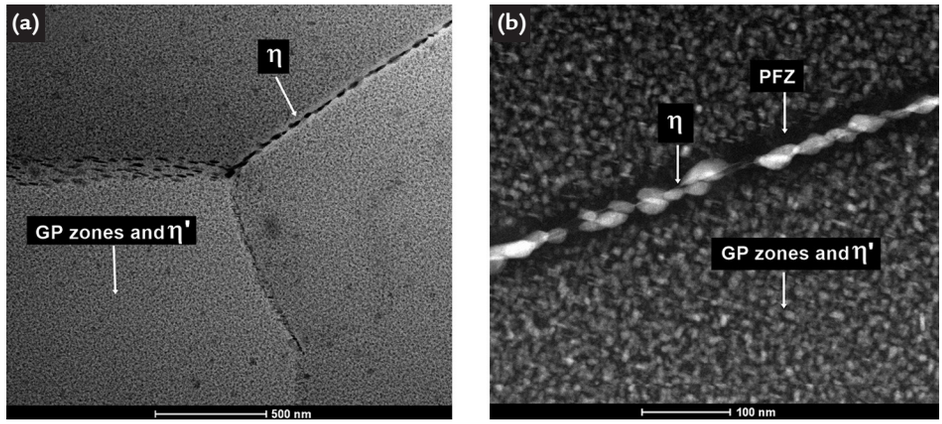

Figure 3
TEM micrographs of (a) and (b) dark field (DF), showing the overall microstructure of the alloy AA7050 in artificially aged T6I4-65 condition, with second phase particles precipitating in the grain boundaries and within the matrix.

Similarly, the condition T6I4-65 showed predominantly fine GPII zones identified as zones homogeneously distributed in the matrix and approximate size of 14 nm; thus, it was confirmed that this condition lies in an underaged state. The difference in sizes of PFZs being 80, 60 and 25 nm for the T7451, T6 and T6I4-65 conditions, respectively is also noticed. It is known that the width of the PFZ influences the loss of ductility; it promotes the heterogeneity of properties in the microstructure, and the matrix has a higher resistance than the grain boundaries (Porter and Easterling, 1996). The results of the microstructure in T6I4-65 condition suggest that it may provide greater resistance to movement of dislocations than larger and more widely spaced precipitates as T7451 and in the T6 temper and, consequently, a higher mechanical resistance, as shown in Lima (2014).

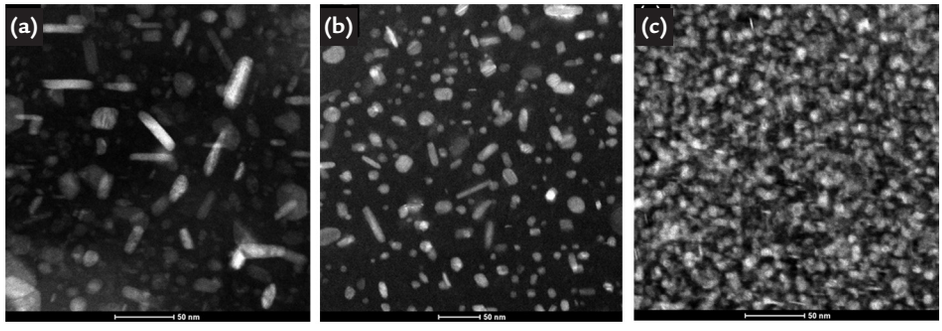

Figure 4
TEM microstructure showing the variation in the volume fraction of precipitates under the conditions (a) T7451, (b) T6 and (c) T6I4-65.

Figures 5 (a), (b) and (c) show the three-dimensional AFM images of the artificially ageing samples obtained from the conditions T7451, T6 and T6I4-65, respectively. The difference can be seen in the surface roughness and precipitate size of the three conditions investigated. It was possible to correlate the density of precipitates with surface roughness found for each condition. Table 3 shows the roughness parameters (Ra) and the measurement of precipitate size detected by AFM. In each case, it proceeded to the overall measurement of a 1x1μm^2 field.

Condition	R_a [nm]	Precipitate size (nm)
T7451	26.6	38 - 641
T6	20.1	24 - 355
T6I4-65	11.7	16 - 196

Table 3
Surface roughness parameters and quantification of the size of precipitate detected by AFM.

The average roughness values (Ra) were obtained from the topographic profile of 3D images of Figures 5 (a), (b) and (c) of T7451, T6 and T6I4-65 conditions, respectively. It is possible to see that the T7451 condition has a rougher surface (R_a: 26.6 nm) compared with T6 (Ra: 20.1 nm) and T6I4-65 (R_a: 11.7 nm).

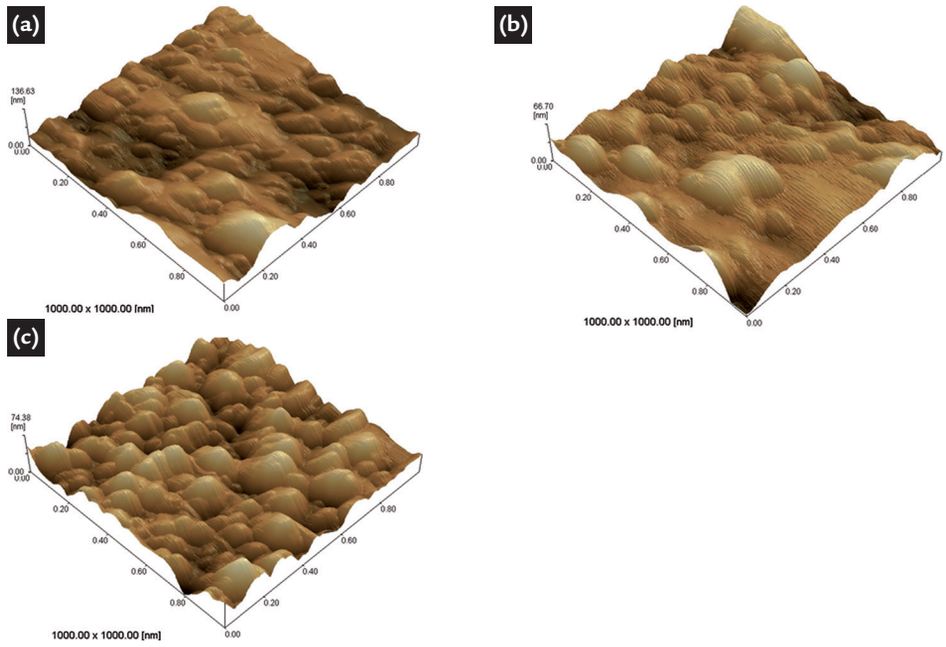

Figure 5
Analysis by AFM topographical showing the surface roughness three-dimensional image of (a) the T7451 condition; (b) the T6 condition; (c) T6I4-65 condition.

The 2D images were used to quantify the minimum and maximum values of precipitate size using the ImageJ software shown in Table 3. It can be seen that the T7451 condition has precipitates with sizes in the range of 38 to 641 nm, which confirms the observed TEM, which revealed particles with an approximate size of 40 nm. A smaller roughness (R_a: 11.7 nm) is associated with larger density of finer precipitates. Whereas, larger precipitates tend to increase the roughness value (R_a = 26.6 nm), as shown in the phase contrast micrograph in Figure 6 (a) which shows lower density of precipitates due to larger particles. While the T6 condition has a roughness R_a = 20.2 nm and precipitate size in the range of 24 to 355 nm, Figure 6 (b) showed an intermediated density of precipitates. The T6I4-65 condition has a roughness R_a = 11.7 nm and particle sizes from 16 to 196 nm and Figure 6 (c) showed a higher density of precipitates.

Moreover, the minimum and maximum values of precipitate size (Table 3) show great scatter for three conditions. It was as consequence of measured intermetallic particles, that likely can contribute to higher scatter. This can be confirmed in Figure 7, which displays the variation of the frequency versus precipitate size in the three ageing conditions in a 1x1μm^2 field. It is possible to notice the absence of greater precipitate size for the three conditions investigated.

The condition T6I4-65 showed a high density of small precipitates, identified as TEM (Figure 3) with GPs zones and η' phase, and homogeneously distributed in the matrix aluminium alloy in relation to the T6 condition that revealed particles of a few nanometers. Figures 7 (a) and (c) indicate that insertion of an interrupted aging stage at 65 °C into a typical T6 heat treatment for aluminium alloy AA7050 that promotes the formation of high density precipitates in the final microstructure.

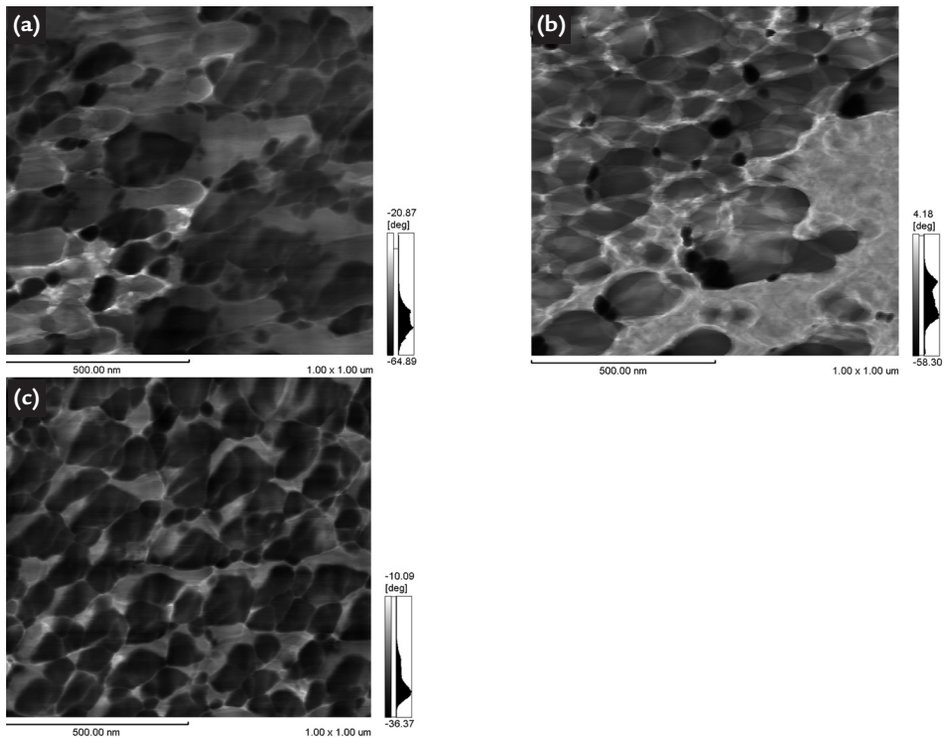

Figure 6
Micrograph AFM, phase contrast, condition (a) T7451, (b) T6 and (c) T6I4-65, revealing the size and density of the precipitates.

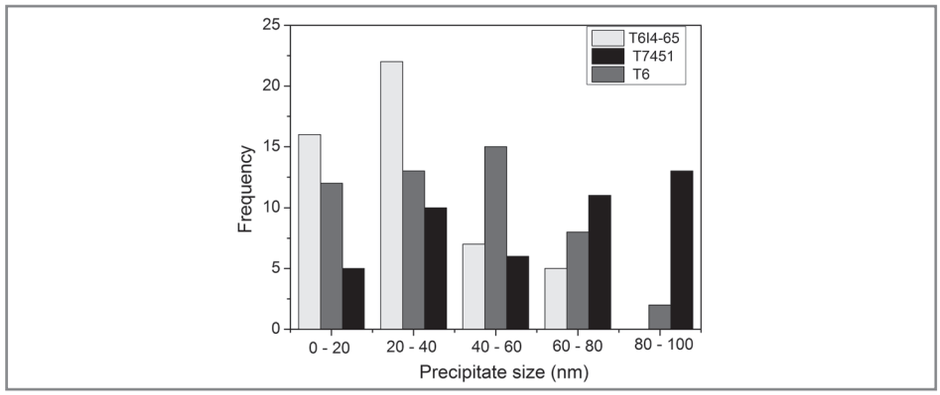

Figure 7
Variation frequency versus precipitate size, on a 1x1μm2 scanned area of the T7451, T6 and T6I4-65 conditions.

Table 4 shows a comparison of the precipitates size obtained by both techniques, TEM and AFM. It is possible to notice the size is less than 30 nm for the η' phase and between 30–200 nm for the η phase; similar results were found by Gjønnes and Simensen, 1970, Deiasi and Adler, 1977, Garcia *et al.*, 2014.

Condition	T7451	T6		T6I4-65	
	η	η'	η	GPs zones	η'
TEM (nm)	38 - 42	17 – 23	45 - 85	14	14
AFM (nm)	38 - 641	24	30 - 355	16	30

Table 4
Quantification of the results of phase η' and η in TEM and AFM.

4. Conclusions

The analysis by AFM allowed a qualitative and quantitative analysis of the surface of the three ageing treatment conditions investigated in this work. Thus, the topographical evaluation results showed an average roughness (Ra) ranging from one condition to the other, as well as a particle size range. This indicated a higher density of small particles evenly distributed in the aluminium alloy matrix in T6I4-65 condition, where it was possible to clearly distinguish the precipitated particles, confirming what was observed in TEM for this condition. However, precautions are needed so that one does not mistake intermetallic particles for precipitates. Thus, the AFM technique proved to be a valid qualitative tool and can complement the results obtained by TEM for exploratory analysis of the microstructure, indicating a new and interesting method to perform the evaluation of the density of nanometric particles. Moreover, the ease of sample preparation consists of basic metallographic techniques not requiring the making of thin films as in TEM, thus allowing the preparation of several samples in a short time.

5. Acknowledgements

The authors acknowledge Coordenação de Aperfeiçoamento de Pessoal de Nível Superior (CAPES) for the financial support, and UEPG – Universidade Estadual de Ponta Grossa for the opportunity and facilities.

6. References

ANDREATTA, F. ***Local Electrochemical Behavior of 7XXX Aluminum Alloys.*** Netherlands:
Netherlands Institute for Metals Research, 2004. 218 f. (DPhil Thesis)

BERG, L. K. et al. GP – zones in Al-Zn-Mg Alloys and their Role in Artificial Aging. ***Acta Materialia.*** v. 49, n. 17, p. 3443-3451, 2001.

BRENT L. A. et al. ***Metallography and Microstructures.*** USA: ASM International, 2004. v. 9, ASM Handbook.

BUHA, J., LUMLEY, R.N., CROSKY, A.G. Microstructural development and mechanical properties of interrupted aged Al-Mg-Si-Cu Alloy. ***Metallurgical and Materials Transactions*** A. v. 37 A, p.3119-3130, 2006.

BUHA, J.; LUMLEY, R.N., CROSKY, A.G. Secondary ageing in an aluminum alloy 7050. ***Materials Science and Engineering,*** v. 492, p. 1–10, 2008.

DEIASI R, ADLER PN. Calorimetric studies of 7000 series aluminum alloys: 1. Matrix precipitate characterization of 7075. ***Metall Trans*** A. v. 8A, n. 7, p 1177–83, 1977.

EPLER, M. Structures by precipitation from solid solution. In ***Metallography and Microstructures***. USA: ASM International, 2004, p. 134–139. v. 9, ASM Handbook.

GARCIA A. L. et al. Comparative quantification and statistical analysis of η′ and η

precipitates in aluminum alloy AA7075-T651 by TEM and AFM. ***Materials Characterization,*** v. 87 p.116 –128, 2014.

GJØNNES J, SIMENSEN CHRJ. An electron microscope investigation of the microstructure in an aluminum-zinc-magnesium alloy. ***Acta Metall,*** v.18, n.8, 881–890, 1970.

KATGERMAN, L., ESKIN, D. Hardening, Annealing, and Aging. In: TOTTEN, G. E., MACKENZIE, D. S. ***Handbook of aluminum: physical metallurgy and process.*** v. 1. New York: Marcel Dekker, 2003. p. 259-303.

LA GARZA et al. Study of precipitates formed in a wrought aluminum alloy by means of atomic force microscopy. ***Materials Characterization*** v.47, p.397– 400, 2002.

LIMA, L. O. R. Study of the effects of two-step ageing heat treatment on fatigue crack growth on an AA7050 aluminum alloy. ***Advance Materials,*** v. 891-892, p.1111-1116, 2014.

PORTER D., EASTERLING K. ***Phase Transformations in metals alloys.*** (2. ed.) Chapman & Hall, 1996. p. 263 – 320.

ROMETSCH P. A., ZHANG Y., KNIGHT, S. Heat treatment of 7xxx series aluminium alloys—Some recent developments. ***Trans. Nonferrous Met. Soc. China,*** v. 24, p. 2003–2017, 2014.

SMALLMAN, R.E., NGAN, A.W. ***Physical metallurgy and advanced materials.*** (7ª ed.) Amsterdam: Elsevier, 2007. 650 p. 385 – 409.

SVERDLIN, A. Introduction to aluminum. In: TOTTEN, G. E., MACKENZIE, D. S. ***Handbook of aluminum: Physical Metallurgy and Process.*** New York: Marcel Dekker, 2003. v. 1, p. 1-32.

Received: 16 February 2016 - Accepted: 25 May 2016.